Journal of Sound and Vibration (2002) **255**(2), 399–406
doi:10.1006/jsvi.2001.4168, available online at http://www.idealibrary.com on IDEAL®

LETTERS TO THE EDITOR

ON THE EXTENSION OF THE INTEGRO-MODAL APPROACH

E. Anyunzoghe

Department of Mechanical Engineering, Laval University, Québec, Canada G1K 7P4

and

L. Cheng

Department of Mechanical Engineering, The Hong Kong Polytechnic University, Hung Hom, Kowloon, Hong Kong. E-mail: mmlcheng@polyu.edu.hk

(*Received* 17 *September* 2001)

1. INTRODUCTION

Prediction of the modal characteristics of acoustic cavities with irregular shapes is an important issue. In many respects, modal pressure (or mode shape) is one of the most essential parameters to be known. First, the mode shape of acoustic cavities is usually used in vibro-acoustic analyses of vibrating structures coupled to an acoustic enclosure [1]. In these cases, the acoustic pressure inside cavities can be decomposed into a series using mode shapes as base functions. Second, problems related to the acoustic intensity inside cavities require an accurate prediction of the velocity of the particles, which is directly related to the sound pressure distribution [2]. Third, accurate information on the mode shape gives rise to many direct applications. For instance, Succi [3] noticed that the position of a minimum resonant pressure in an automobile cabin can be changed, so as to improve the driver's and the passengers' comfort. All these applications are based on an accurate prediction of the modal sound distribution.

In our previous work [4], an integro-modal approach (IMA) was suggested to compute the acoustic modal properties of irregular cavities, where the separation of variable technique cannot be applied. This previous work mainly focused on predicting the natural frequencies. No study in terms of the corresponding modal pressures was performed. It consisted of handling the irregular-shaped enclosure as a multi-connected cavity system. For each sub-cavity, rigid-wall modes were used as base functions for a modal expansion of the sound field. The integral formulation ensured global continuity of the pressure between adjacent sub-cavities. In different studies, Pan [5–7] pointed out that using a rigid-wall mode expansion for the sound field does not always describe correctly the particle velocity or pressure gradient where absorptive or flexible part of the cavity boundary is assumed. The convergence of the acoustic pressure may also be affected in the whole cavity. This problem is likely to occur when the IMA is applied.

This issue is discussed in the present paper. Using a simple semi-circular cavity, the performance of the original IMA in terms of prediction of the sound pressure distribution is first discussed. Based on the problem observed, an improved IMA based on the use of overlapped cavities is proposed. It can be shown that this technique can greatly improve the accuracy of the prediction for the modal pressure and velocity distribution.

0022-460X/02/$35.00

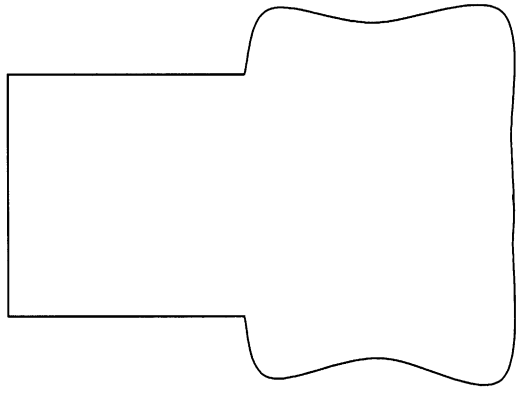

Figure 1. Irregular-shaped cavity

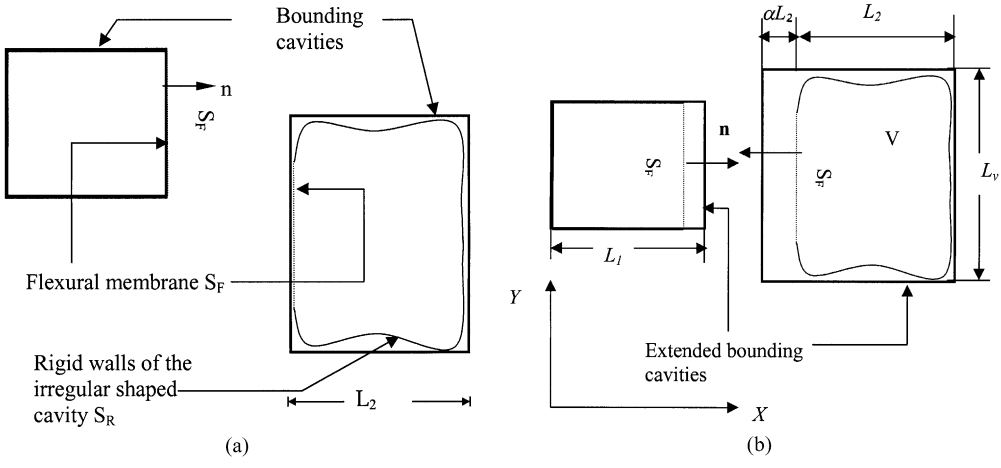

Figure 2. Discretization of the IMA. (a) Original approach, (b) improved approach with overlapped cavities.

2. THEORETICAL DEVELOPMENT

Figure 1 shows a typical cavity comprising a regular-shaped part and an irregular-shaped part. The original IMA handles the whole cavity as a sum of two or more connected sub-cavities, regular or not, separated by a virtual membrane S_F, as shown in Figure 2a. The modal characteristics of regular sub-cavities were obtained analytically, while irregular ones were treated using normal modes of their respective regular bounding cavities with rigid walls. In both cases, rigid-walled modes were used as base functions for a modal expansion of the sound field in the sub-cavity. An integral formulation ensured global continuity of the pressure between adjacent sub-cavities. The method then yielded a truncated eigenvalue system. The use of rigid-walled modes will therefore impose a systematic zero pressure gradient over the junction area, leading inevitably to an error in the sound pressure calculation. To overcome this obstacle, the present paper suggests lengthening the bounding cavity so that its boundary does not cover the membrane surfaces S_F, but permitting a certain degree of overlapping. α is defined as the ratio of the additional length to the original length (related to the original approach) of the bounding cavity in the

direction normal to the separating membrane surfaces (Figure 2b). Whereas adjacent bounding cavities were previously stuck together along their connecting surfaces in the original approach, a slight overlap is allowed among them in the new approach, because of which α is called the overlapping ratio.

In two-dimensional cases, the bounding cavity may be rectangular, circular, or of any other shape as far its modal characteristics are known. To ensure good accuracy, the selected bounding cavity must fit, as much as possible, the geometrical shape of its corresponding enclosed sub-cavity. Rectangular bounding cavities are the easiest to handle in practice. Taking it as an example, the following sections briefly summarize the formulation of the improved IMA.

In each sub-volume V, the interior pressure Ψ satisfies the Green's integral equation with associated boundary conditions on the enclosing surface S

$$\Psi(r) = \int_S \left(G(r, r_o) \frac{\partial \Psi(r_o)}{\partial n} - \Psi(r_o) \frac{\partial G(r, r_o)}{\partial n} \right) \mathrm{d}S \tag{1}$$

r and r_o are the observation and source points in the cavity respectively. The boundary conditions over the flexible membrane are determined by continuity of the normal air particle velocity and the structural velocity on the separating surface, noted as S_F. Hence,

$$\partial \Psi / \partial n = -\rho_f \ddot{w} \quad \text{on } S_F, \tag{2}$$

where n is the normal to the surface of the boundary (positive outwards) and w is the flexural displacement of the separating membrane. ρ_f is the air density within the cavity. The flexible portion of S refers only to the separating membrane between two adjacent sub-cavities. Anywhere else on the remaining surface, the pressure gradient is zero.

Each sub-volume is treated separately. To construct the Green function G and the solution, the initial sub-volume V is enclosed in a larger bounding volume V_b (Figure 2b), of standard geometry and with rigid walls S_b. The modal characteristics (Φ_N, ω_N) of V_b are obtained analytically to express the Green function G [8]. Using the same modal functions, Ψ can be expressed as follows:

$$\Psi(r, t) = \rho_f c_f^2 \sum_n \frac{a_n(t)}{\Lambda_n} \Phi_n(r), \tag{3}$$

where c_f is the speed of sound in air, Λ_n the generalized mass of the nth normal mode of V_b and a_n the unknown coefficients. Similarly, the flexural displacement of the vibrating membrane w can be expanded in terms of *in vacuo* normal mode shapes φ_m defined over the region S_F:

$$w = \sum_m q_m(t) \varphi_m, \tag{4}$$

where m is the structural modal indices, $q_m(t)$ are the structural modal co-ordinates. Assume

$$a_n(t) = a_n \mathrm{e}^{\mathrm{i}\omega t}. \tag{5}$$

Knowing the orthogonal properties of the base functions, and the boundary conditions, and using the modal expansions in equations (1) and (2), the integral equation equation (1)

becomes:

$$(\omega_n^2 - \omega^2)\, a_n + \frac{c^2}{V} \sum_{n'} \frac{a_{n'}}{\Lambda_{n'}}\, T_{n',n} = \omega^2 \frac{S_f}{V_b} \sum_m q_m L_{nm}, \tag{6}$$

$$T_{n',n} = \int_S \Phi_{n'} \frac{\partial \Phi_n}{\partial n}\, \mathrm{d}s, \qquad L_{nm} = \frac{1}{S_F} \int_{S_F} \Phi_n(r_o^S)\, \varphi_m(r_o^S)\, \mathrm{d}S, \tag{7}$$

where $T_{n',n}$ is the spatial coupling coefficient between the nth and the n'th acoustic modes of the bounding cavity and L_{nm}, the spatial modal coupling coefficient between the mth structural mode and the nth acoustic mode.

Furthermore, by assuming a mass-less and stiffness-free membrane, it was demonstrated that the equation describing the flexural motion of the separating membrane is reduced to the following [4]:

$$\int_{S_F} \Psi^+ \varphi_m\, \mathrm{d}s - \int_{S_F} \Psi^- \varphi_m\, \mathrm{d}s = 0, \tag{8}$$

where Ψ^+ and Ψ^- are the sound pressure at each side of the membrane. It can be noticed that the above expression represents a global continuity of the pressure due to the integrals involved and therefore indicates a pure opening between two adjacent sub-cavities.

The integrals are computed for a rectangular bounding cavity of dimensions $L_y \times (1 + \alpha) L_1$ and $L_y \times (1 + \alpha) L_2$ ($\alpha = 0$ represents the real rectangular sub-cavity of dimension $L_y \times (L_1 + L_2)$). In Cartesian co-ordinates, the connecting membrane is defined by the equation $x = L_1$. The first sub-cavity will have the following modes and properties:

$$\Phi_n(x, y) = \cos\left(\frac{n_x \pi x}{(1 + \alpha) L_1}\right) \times \cos\left(\frac{n_y \pi y}{L_y}\right). \tag{9}$$

Then the coupling coefficient between nth mode and the n'th mode in equation (7) can be calculated as

$$T_{n',n} = \frac{n_x \pi L_y}{(1 + \alpha) L_1} \times \sin\left(\frac{n_x \pi}{1 + \alpha}\right) \times \left(\frac{1}{2} + \frac{1}{2}\, \delta_{0,n_y}\right) \delta_{n'_y,n_y}. \tag{10}$$

If $\alpha = 0$, $T_{n,n'} = 0$, thus, the addition of α has the effect of coupling the acoustic modes of the bounding cavities in their respective enclosed sub-cavities.

The flexural displacement of the flexible membrane can be represented by any set of orthogonal functions provided that they are complete in the region of the membrane surface. Assuming

$$\varphi_m(y) = \sin\left(\frac{m \pi y}{L_y}\right), \tag{11}$$

it can be shown that

$$L_{nm} = -\cos\left(\frac{n_x \pi}{1 + \alpha}\right) \times \frac{m((-1)^{n_y + m} - 1)}{\pi (n_y^2 - m^2)} L_y \quad \text{if } n \neq m;$$

$$L_{nm} = 0 \quad \text{if } n_y = m \quad \text{or} \quad n_y = 0. \tag{12}$$

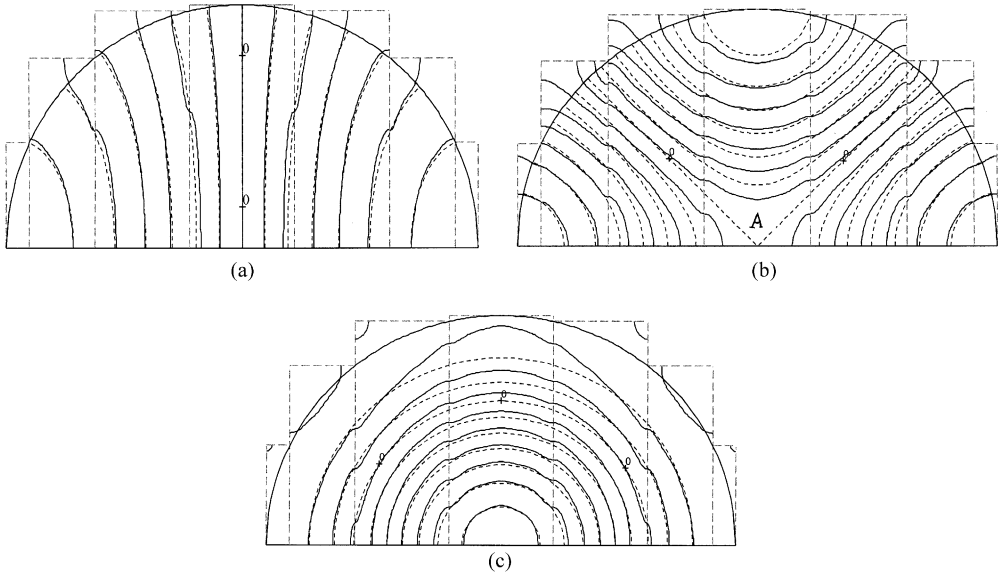

Figure 3. Lines of constant acoustic pressure amplitude (normalized to maximum value). ----, Theoretical results; ———, original IMA results. (a) Mode (1, 0); (b) Mode (2, 0); (c) Mode (0, 1).

The key relations for solving the internal acoustic distribution in the cavity are equations (6) and (8). These coupled acoustic-structural equations form an eigenvalue system, ω^2 being the unknown eigenvalue. For each eigenvalue, there is a corresponding eigenvector given by the coefficients a_n and q_m, which can then be used to compute the acoustic pressure distribution inside the cavity. All series expansions used in the calculations of G, Ψ and w have to be truncated, in order to implement a numerical procedure.

It should be pointed out that this formulation is more general than the original IMA formulation in the sense that taking $\alpha = 0$ leads us back to the original approach.

3. NUMERICAL RESULTS USING A SEMI-CIRCULAR CAVITY

A simple semi-circular cavity is first used to test the method. Analytical solutions available for this configuration provide a good basis for comparison purposes. Actually, the analysis for this simple model will mostly focus on the prediction of the modal pressure distribution mainly in the vicinity of connecting surfaces. A semi-circular enclosure of radius 1 m is considered. An exact solution can be obtained by solving the Helmholtz equation using the method of separation of variables in polar co-ordinates. Calculations give lines of constant acoustic pressure amplitude in the semi-circular cavity for the first three natural modes. The pressure amplitude has been normalized by its maximum value in the cavity and the pressure variation between two successive lines is 0·15 units. Firstly, a zero overlapping ratio was assumed with seven acoustic and membrane modes and seven sub-divisions. In Figure 3(a)–3(c), theoretical results are designated by dotted lines and original IMA results by solid lines. Agreement with analytical results is good especially for the first degenerated mode (1, 0). This particular mode resembles the (1, 0) mode of a rectangular cavity, with the exception of the lines of constant pressure being slightly curved in this case and adjusting themselves to meet the homogeneous boundary conditions

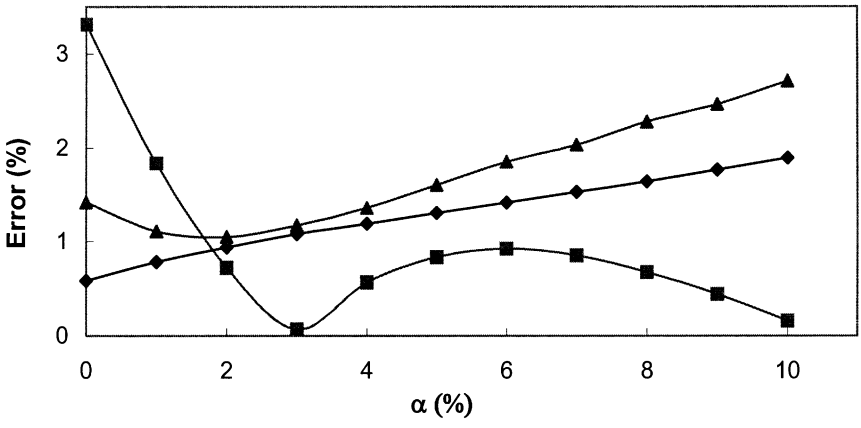

Figure 4. Averaged sound pressure error inside the cavity versus different α values. —◆—, Mode (1, 0); —■—, Mode (2, 0); —▲—, Mode (0, 1).

along the circular edge of the cavity. The lines outside the cavity have no physical significance, but they illustrate how the method works, i.e., approximates the acoustic pressure using rigid-wall modes of rectangular sub-cavities. As expected, numerical solutions reveal discontinuous slopes of the acoustic pressure lines across the connecting panels. The generated error between the numerical and the analytical solutions is increased in the vicinity of such areas and propagates eventually in the entire cavity. Figure 3(b) corresponds to the second mode of order (2, 0). The numerical solution fails to give an accurate approximation of the pressure amplitude near point "A" (specified in Figure 3(b)) which is a singular point in polar co-ordinates, for this particular mode. When detail near that point is required, one may increase the number of acoustics modes in the series expansion. But according to the present approach, it is first suggested to use the technique of overlapped cavities without increasing either the number of sub-cavities, or the number of acoustic and membrane modes, Similar phenomena can be observed in Figure 3(c) for the third mode. Again, improvement is needed to increase the accuracy of the method.

In order to investigate the influence of the non-zero overlapping ratio on the acoustic pressure estimation for each point in the cavity, different α values are first tested. To this end, the average sound pressure inside the cavity is calculated. The error is calculated and expressed in percentage compared to the analytical solution for the first three modes. Figure 4 shows the result. Since the original approach already gives acceptable results as shown in Figure 3(a), using overlapped cavities cannot bring about any further improvement. For the two other modes, however, optimal α value seems to be somewhere between 2 and 3%. Beyond that, the bounding cavities are too distorted from the real sub-cavities to give a reasonable approximation.

Using $\alpha = 3\%$, detailed results on sound pressure distribution are given in Figure 5(a)–5(c). These three figures can be compared to their zero-ratio equivalent given in Figure 3(a)–3(c). In Figure 3(a) the original approach already gives a good approximation of the first mode. Figure 5(a) shows that overlapped cavities can still bring about further improvement. While the predicted local pressure still agrees very well with the analytical solution, the curving of the pressure amplitude lines is apparently much smoother compared to Figure 3(a) (when $\alpha = 0$). The pressure gradient across the opening membranes agrees more with the expected solution than the previous case.

The most compelling enhancement is achieved for the second mode, for which $\alpha = 3\%$ leads almost to the exact resolution (Figure 5(b)). The agreement of the local pressure with

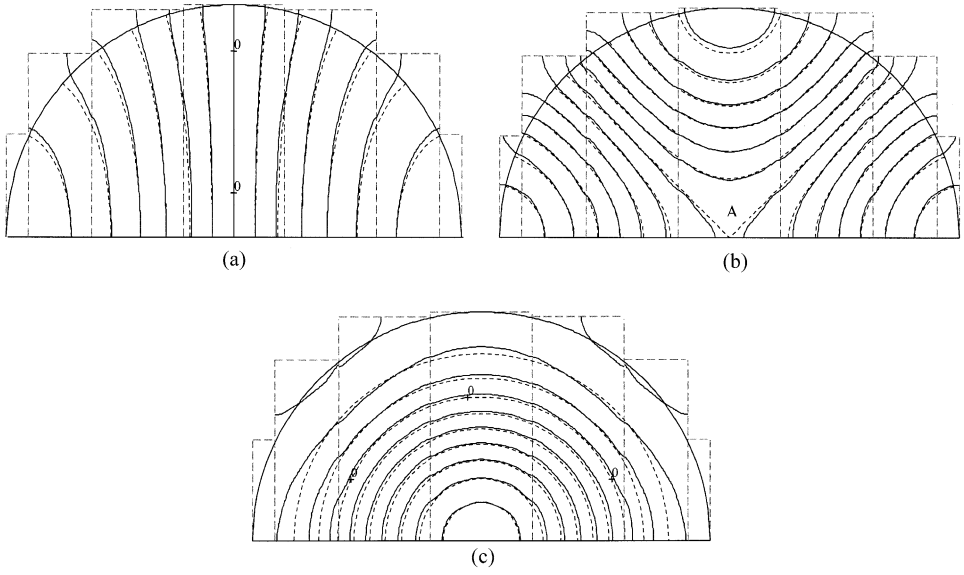

Figure 5. Lines of constant acoustic pressure amplitude (normalized to maximum value). ----, Theoretical results; ———, improved IMA results with $\alpha = 3\%$. (a) Mode (1, 0); (b) Mode (2, 0); (c) Mode (0, 1).

exact distribution is excellent everywhere in the cavity, even near the singular point A. Calculated lines of constant pressure match with the theoretical lines along opening surfaces and the rigid boundary of the cavity. The pressure gradient is fairly continuous. Looking at the pressure distribution of the third mode (Figure 5(c)), again comparisons with the zero-ratio resolution show reasonable improvement. It should be emphasized that the original approach with $\alpha = 0\%$ would have required much more acoustic modes and sub-cavities to obtain the comparable result. Thus, the benefit of the overlapping technique can be twofold: solving the problem of inhomogeneous condition across the flexural membranes surface, and improving the convergence using minimum decomposition terms.

4. CONCLUSIONS

The technique based on the use of an overlapping ratio is efficient to solve or at least to attenuate the problem of gradient discontinuity between adjacent sub-cavities encountered in the original IMA without altering the good accuracy in the frequency estimation. Satisfactory results can be achieved with very limited number of acoustic modes in the series expansion. To determine the optimal value of the overlapping rate, however, successive numerical tests may be necessary.

REFERENCES

1. J. MISSAOUI and L. CHENG 1999 *Journal of Sound and Vibration* **226**, 101–123. Vibroacoustic analysis of a finite cylindrical shell with a floor partition.
2. L. CHENG and J. NICOLAS 1992 *Journal of the Acoustical Society of America* **91**, 1504–1513. Radiation of sound into a circular cylindrical enclosure from point-driven plates with general boundary conditions.
3. G. P. SUCCI 1987 *Journal of the Acoustical Society of America* **81**, 1688–1694. The interior acoustic field of an automobile cabin.

4. J. MISSAOUI and L. CHENG 1997 *Journal of the Acoustical Society of America* **101**, 3313–3321. A combined integro-modal approach for predicting acoustic properties of irregular-shaped cavities.
5. J. PAN and D. A. BIES 1990 *Journal of the Acoustical Society of America* **87**, 691–707. The effect of fluid–structural coupling on sound waves in an enclosure—theoretical part.
6. J. PAN 1993 *Journal of the Acoustical Society of America* **93**, 1641–1644. A note on the prediction of sound intensity.
7. J. PAN 1995 *Journal of the Acoustical Society of America* **97**, 691–694. A second note on the prediction of sound intensity.
8. A. D. PIERCE 1981 *Acoustics*: *An Introduction to its Physical Principles and Applications*. New York: McGraw-Hill.